Journal of Inclusion Phenomena and Macrocyclic Chemistry **42:** 301–311, 2002.

Rotaxane Type Complexation Behavior of Cyclodextrins with Zinc (II) Tetraphenylporphyrin-Viologen Linked Compounds

TOMOMI UJIIE, TATSUYA MOROZUMI, TAKASHI KIMURA, TOSHIYUKI ITO and HIROSHI NAKAMURA*

Division of Material Science, Graduate School of Environmental Earth Science, Hokkaido University, Sapporo 060-0810, Japan

(Received: 7 August 2001; in final form: 18 December 2001)

Key words: rotaxane type complexation, supramolecular structure, cyclodextrins, zinc (II) tetraphenylporphyrin-viologen linked compounds

Abstract

The complexation behavior of zinc (II) tetraphenylporphyrin-viologen covalently linked compounds by a polymethylene chain ($ZnPC_nV^{2+}$; $n = 4$–9) with tri-*O*-methyl-β-cyclodextrin (TM-β-CD) was investigated by means of ^{1}H NMR and UV/Vis absorption spectrometry in acetonitrile-water (1:1, v/v). The ^{1}H NMR spectra indicated that $ZnPC_nV^{2+}$ existed as a mixture of a dimer and a monomer at high concentration ($>1 \times 10^{-3}$ M). The dimer was degraded to the monomer upon complexation with TM-β-CD involving the formation of 1:1 and 1:2 ($ZnPC_nV^{2+}$: TM-β-CD) complexes, which was observed by UV/Vis spectrometry. Furthermore, ^{1}H NMR spectra exhibited that there are at least two types of structures for these complexes, one is a fast exchanging complex, and another is a slow exchanging one. A slow exchanging complex could be assigned as a rotaxane type structure in which the methylene chain moiety of $ZnPC_nV^{2+}$ penetrated into the cavity of TM-β-CD. Discrete formation constants for these complexes were evaluated. The values were little affected by the spacer methylene chain length ($n \geq 7$).

Introduction

Cyclodextrins (CDs) are well known as host molecules that have an ability to produce supramolecular complexes with many organic compounds in aqueous solution [1, 2]. To extend their ability, various photo reactive groups, or electron acceptors, have been attached to the CDs, and efficient photoinduced electron transfers or energy transfers between the CD-appended moieties and guest molecules included in the cavity of the CDs have been demonstrated [3–9]. Especially, zinc (II) tetraphenylporphyrin (ZnTPP) has been much attracted as a photosensitizer for the oxidation of water in an artificial photosynthesis system. Therefore, the inclusion phenomena into a CD cavity of ZnTPP derivatives were widely studied and the structure unit in the artificial photosynthetic catalyst based on CD. Lawrence *et al.* [10, 11] and Nolte *et al.* [12] reported the inclusion behavior of water-soluble TPP with CD for the construction of heme-dependent protein mimics. The photochemical study of water-soluble TPP·CD was also carried out by Mosseri *et al.* [13].

The TPP molecules were also employed as a part of electron donor-acceptor (D-A) coverently linked compounds, which has been one of the most popular research subjects relevant to artificial photosynthesis [14–16]. For the purpose of constructing the efficient photo energy conversion systems, a large number of experimental and theoretical investigations have been carried out to elucidate the role of the spacer between D and A in the long range electron transfer processes [14–18]. With the aid of several microenvironments and external perturbation such as electric fields or magnetic fields, the controls of photoinduced electron transfer have been successful in several D-A systems [19, 20]. In this context, we and other research groups have been studying the behavior of photo induced charge transfer in ZnTPP-viologen linked molecule in various media [21–25].

The preparation of D-A linked compounds with a flexible polymethylene chain, $-(CH_2)_n-$, is easier than molecules with a rigid bridge. The study on the distance dependence of the electron transfer rates in the D-A linked compounds with a flexible bridge usually give complicated results due to a distribution of different conformations even in molecular assemblies. To avoid this, one suitable idea was to construct a rotaxane type molecule using CD.

Recently, supramolecular chemistry such as catenanes and rotaxanes with CDs attracts considerable interest from many researchers [26–28]. Catenanes and rotaxanes are mechanically interlocked compounds that incorporate CDs as one of their components. These rotaxane-type cyclodextrin complexes have been studied intensively as one of the most important supramolecular assemblies in various fields [29, 30]. In spite of the fast growing report concerned with CD, only a few studies involving a D-A·CD rotaxane

* Author for correspondence.

type complex have been published. Matsuo and his coworkers have reported the formation of stable rotaxane type supramolecular complexes in several aromatic D-A linked compounds, such as phenothiazine- [31–34], carbazole- [35, 36] and anthracene-viologen [37] linked systems in water. Other research groups have also reported the rotaxane type supramolecular complexes of ruthenium trisbipyridine- [38] or naphthalene derivatives-viologen [39] linked compounds with β-CD in aqueous medium.

The D-A molecules usually have low solubility in water whereas the CDs are not soluble in many organic solvents. To overcome this defect, the use of *O*-methylated CDs [40–44] are more suitable in many investigations due to the solubility in various organic solvents compared with native CDs [45]. The dimethylated β-CD (DM-β-CD) complexes usually gave complex ^{1}H NMR spectra, because pure DM-β-CD is difficult to obtain due to the existence of many isomers in the *O*-methyl positions. On the other hand, pure per-methylated β-CD (i.e., TM-β-CD) gave simpler NMR spectra. In this paper, the complexation behavior of zinc (II) porphyrin-viologen linked compounds ($ZnPC_nV^{2+}$) with 2,3,6-tri-*O*-methyl-β-CD (TM-β-CD) was investigated in acetonitrile-water by ^{1}H NMR and UV/Vis absorption spectrometry.

Experimental section

Apparatus

^{1}H NMR spectra (400 MHz) were measured with a JEOL EX-400 ^{1}H NMR spectrometer, and UV/Vis absorption spectra were recorded with a Shimadzu UV-2400PC spectrophotometer. In all measurements, the temperature was maintained at 30 ± 0.2 °C for ^{1}H NMR and at 25 ± 0.1 °C for UV/Visible spectra. The chemical shifts of the ^{1}H NMR spectra of $ZnPC_nV$ in $CDCl_3$–CD_3OD (9:1,v/v), given in this Experimental section, were quite sensitive to the composition of the solvent and also to the concentration of the compounds. So, the chemical shifts of these compounds in this section are not precise.

Materials

All organic compounds for the syntheses of $ZnPC_nV$ were commercially available and used without further purification. Acetonitrile (CH_3CN) was purchased from Dojindo (spectrophotometric grade) and used without further purification. Water was purified by distillation twice. 2,3,6-Tri-*O*-methyl-β-cyclodextrin (TM-β-CD) was purchased from Nacalai Tesque, Inc. and used without further purification.

Syntheses of reagents

5-(4-Hydroxyphenyl)-10,15,20-triphenyl-21H,23H-porphin (H_2TPPOH). Pyrrole (20.2 g, 0.3 mol) was added to a solution of 4-hydroxybenzaldehyde (9.2 g, 0.075 mol), benzaldehyde (23.8 g, 0.225 mol) in propionic acid (500 mL), and the mixture was refluxed for 3 h. A large amount of methanol was added after most of the propionic acid was removed by distillation under reduced pressure. The resultant black solids were collected by filtration and washed with methanol several times. Yield (crude): 6.6 g (35%). This crude compound was a mixture of porphyrins with several hydroxy groups, and was purified in the following steps.

Zinc 5-(4-hydroxyphenyl)-10,15,20-triphenylporphinate (ZnTPPOH). To incorporate zinc ion into the porphyrin center, zinc acetate (45 g, 0.245 mol) in methanol (200 mL) was added to the solution of H_2TPPOH (6.6 g, 9.5 mmol) in chloroform–methanol (7:3, v/v, 500 mL), and was refluxed for 4 h. After evaporation of the solvent, the residue was dissolved in chloroform and excess zinc acetate filtered off. The filtrate was concentrated and purified by chromatography on a silica gel column (Wakogel C-200) (eluent: $CHCl_3$). The second fraction was collected and concentrated. This purification was repeated once more. The corresponding fraction was concentrated, and hexane was added for reprecipitation and the resulting purple solid was collected by filtration. Yield: 1.86 g (9.9 %). ^{1}H NMR ($CDCl_3$) δ = 5.09 (1H, s; –OH), 7.20 (2H, d; aromatic), 7.72–7.78 (9H, m; aromatic), 8.08 (2H, d; aromatic), 8.27 (6H, m; aromatic), 8.94–8.99 (8H, m; aromatic). Found: C, 73.59; H, 4.23; N, 7.93%; C/N, 9.28. Calcd. for $C_{44}H_{28}N_4OZn$: C, 76.13; H, 4.07; N, 8.07%; C/N, 9.43.

Zinc 5-(4-(ω-bromoalkyloxy)phenyl)-10,15,20-triphenylporphinate ($ZnPC_nBr$). Typical procedure of syntheses of $ZnPC_nBr$ is as follows (e.g., n = 8): ZnTPPOH (0.41 g, 0.58 mmol), 1,8-dibromooctane (2 g, 8.0 mmol), and potassium carbonate (1.2 g, 8.8 mmol) were suspended in dry *N*,*N*-dimethylformamide (40 mL) and stirred for 40 h at room temperature. After the solvent was evaporated under reduced pressure, the residue was dissolved in $CHCl_3$ and washed with water. The organic layer was dried over magnesium sulfate, and evaporated to remove the solvent. The residue was purified by chromatography on a silica gel column (Wakogel C-200) (eluent: $CHCl_3$). The first fraction was collected. This fraction was concentrated, and hexane was added for reprecipitation and the resulting purple solid was obtained by filtration.

$ZnPC_8Br$. Yield: 0.43 g (84 %). ^{1}H NMR ($CDCl_3$) δ = 1.48–1.68 (8H, m; $-CH_2-$), 1.89–2.02 (4H, m; $-CH_2-$), 3.46 (2H, t; $-CH_2Br$), 4.25 (4H, t; $-OCH_2-$), 7.72–7.77 (9H, m; aromatic), 8.11 (2H, d; aromatic), 8.22 (6H, m; aromatic), 8.93–8.99 (8H, m; aromatic). Found: C, 70.43; H, 4.96; N, 6.58%; C/N, 10.70. Calcd. for $C_{52}H_{43}N_4OZnBr$: C, 70.56; H, 4.90; N, 6.33%; C/N, 11.15.

$ZnPC_4Br$. Yield: 0.35 g (75%). ^{1}H NMR ($CDCl_3$) δ = 2.13–2.30 (4H, m; $-CH_2-$), 3.63 (2H, t; $-CH_2Br$), 4.30 (2H, t; $-OCH_2-$), 7.26 (2H, d; aromatic), 7.72–7.79 (9H, m; aromatic), 8.12 (2H, d; aromatic), 8.22 (6H, m; aromatic), 8.94–8.99 (8H, m; aromatic). Found: C, 70.10; H, 4.67; N,

6.85%; C/N, 10.23. Calcd. for $C_{48}H_{35}N_4OZnBr$: C, 69.53; H, 4.26; N, 6.76%; C/N, 10.29.

ZnPC$_5$Br. Yield; 0.23 g (48%). ^{1}H NMR ($CDCl_3$) δ = 1.79–1.83 (2H, m; –CH_2–), 2.00–2.04 (2H, m; –CH_2–), 2.06–2.10 (2H, m; –CH_2–), 3.54 (2H, t; –CH_2Br), 4.27 (2H, t; –OCH_2–), 7.27 (2H, d; aromatic), 7.72–7.79 (9H, m; aromatic), 8.11 (2H, d; aromatic), 8.21 (6H, m; aromatic), 8.93–8.99 (8H, m; aromatic). Found: C, 68.04; H, 4.68; N, 6.37%; C/N, 10.68. Calcd. for $C_{49}H_{37}N_4OZnBr{\cdot}H_2O$: C, 68.30; H, 4.56; N, 6.51%; C/N, 10.51.

ZnPC$_6$Br. Yield: 0.47 g (94 %). ^{1}H NMR ($CDCl_3$) δ = 1.66–1.68 (4H, m; –CH_2–), 1.97–2.04 (4H, m; –CH_2–), 3.51 (2H, t; –CH_2Br), 4.26 (2H, t; –OCH_2–), 7.27 (2H, d; aromatic), 7.72–7.79 (9H, m; aromatic), 8.11 (2H, d; aromatic), 8.22 (6H, m; aromatic), 8.93–9.00 (8H, m; aromatic). Found: C, 70.68; H, 5.55; N, 6.13%; C/N, 11.53. Calcd. for $C_{50}H_{39}N_4OZnBr$: C, 70.06; H, 4.59; N, 6.54%; C/N, 10.71.

ZnPC$_7$Br. Yield: 0.41 g (82%). ^{1}H NMR ($CDCl_3$) δ = 1.55–1.68 (6H, m; –CH_2–), 1.95–2.00 (4H, m; –CH_2–), 3.48 (2H, t; –CH_2Br), 4.26 (2H, t; –OCH_2–), 7.27 (2H, d; aromatic), 7.73–7.78 (9H, m; aromatic), 8.11 (2H, d; aromatic), 8.22 (6H, m; aromatic), 8.94–9.00 (8H, m; aromatic). Found: C, 71.31; H, 5.25; N, 6.60%; C/N, 10.80. Calcd. for $C_{51}H_{41}N_4OZnBr$: C, 70.31; H, 4.74; N, 6.43%; C/N, 10.90.

ZnPC$_9$Br. Yield: 0.49 g (86%). ^{1}H NMR ($CDCl_3$) δ = 1.43–1.64 (10H, m; –CH_2–), 1.89–2.02 (4H, m; –CH_2–), 3.45 (2H, t; –CH_2Br), 4.27 (2H, t; –OCH_2–), 7.27 (2H, d; aromatic), 7.74–7.76 (9H, m; aromatic), 8.11 (2H, d; aromatic), 8.22 (6H, m; aromatic), 8.93–8.99 (8H, m; aromatic). Found: C, 70.74; H, 5.05; N, 6.30%; C/N, 11.22. Calcd. for $C_{53}H_{45}N_4OZnBr$: C, 70.79; H, 5.04; N, 6.23%; C/N, 11.36.

N-propyl-4,4′-bipyridinium bromide (C_3bpy). A mixture of 4,4′-bipyridine (28 g, 0.18 mol) and 1-bromopropane (7.3 g, 0.053 mol) in dry CH_3CN (200 mL) was refluxed for 28 h. The solvent was removed, and the resulting yellow solid was extracted with diethylether by Soxhlet extractor for 12 h. The residual solid was used for further reactions. Yield: 14.6 g (98.6%). ^{1}H NMR ($CDCl_3$) δ = 1.07 (3H, t; –CH_3), 2.11–2.20 (2H, m; –CH_2–), 5.05 (2H, t; N–CH_2–), 7.69 (2H, d; aromatic), 8.35 (2H, d; aromatic), 8.89 (2H, d; aromatic), 9.65 (2H, d; aromatic). Found: C, 55.44; H, 5.44; N, 9.95%; C/N, 5.57. Calcd. for $C_{13}H_{15}N_2Br$: C, 55.93; H, 5.42; N, 10.04%; C/N, 5.57.

N-(4-(Zinc 10,15,20-triphenylporphin-5-yl)phenyl)-N′-propyl-4,4′-bipyridinium bromide (ZnPC$_n$V). Typical procedure of syntheses of ZnPC$_n$V (for example, n = 8) is as follows: A mixture of ZnPC$_8$Br (0.26 g, 0.28 mmol) and C_3bpy (1.0 g, 2.6 mmol) in dry *N,N*-dimethylformamide was stirred over 3 days at 80 °C. After the solvent was removed under reduced pressure, the residue was dissolved in chloroform and washed with aqueous 1.5 M potassium bromide three times. The solvent was removed and the residue was purified by gel permeation chromatography (Sephadex LH-20) with methanol as an eluent, twice. The main fraction was collected and the solvent was removed. The residue was dissolved in a small portion of chloroform-methanol mixed solvent (10:1, v/v), and then hexane was added for reprecipitation and the purple precipitates were collected by filtration.

ZnPC$_8$V. Yield: 0.10 g (30.4%). ^{1}H NMR ($CDCl_3$–CD_3OD(9:1, v/v)) δ = 1.03 (3H, t; –CH_3), 1.60–1.69 (8H, m; –CH_2–), 2.09–2.18 (6H, m; –CH_2–), 4.26 (2H, t; –OCH_2–), 4.53 (2H, t; –NCH_2–), 4.75 (2H, t; –NCH_2–), 7.26 (2H, d; aromatic), 7.75 (9H, m; aromatic), 8.08 - 8.10 (2H, d; aromatic), 8.20–8.21 (6H, m; aromatic), 8.66 (2H, d; aromatic), 8.74 (2H, d; aromatic), 8.86–8.93 (8H, m; aromatic), 9.01 (2H, d; aromatic), 9.21 (2H, d; aromatic). Found: C, 63.83; H, 5.12; N, 6.90%; C/N, 9.25. Calcd for $C_{65}H_{58}N_6OZnBr_2{\cdot}3H_2O$: C, 64.07; H, 5.29; N, 6.90%; C/N, 9.29.

ZnPC$_4$V. Yield: 0.27 g (82.2%). ^{1}H NMR ($CDCl_3$–CD_3OD(9:1, v/v)) δ = 1.04 (3H, t; –CH_3), 2.06 (2H, m; –CH_2–), 2.18–2.52 (4H, m; –CH_2–), 4.36 (2H, t; –OCH_2–), 4.58 (2H, t; –NCH_2–), 4.99 (2H, t; –NCH_2–), 7.26 (2H, d; aromatic), 7.73 (9H, m; aromatic), 8.12 (2H, d; aromatic), 8.21 (6H, m; aromatic), 8.75 (2H, d; aromatic), 8.82 (2H, d; aromatic), 8.87–8.88 (8H, m; aromatic), 9.12 (2H, d; aromatic), 9.36 (2H, d; aromatic). Found: C, 63.11; H, 5.01; N, 7.12%; C/N, 8.72. Calcd. for $C_{61}H_{50}N_6OZnBr_2{\cdot}3H_2O$: C, 63.04; H, 4.86; N, 7.23%; C/N, 8.72.

ZnPC$_5$V. Yield: 0.28 g (93.4%). ^{1}H NMR ($CDCl_3$–CD3OD(9:1, v/v)) δ = 1.02 (3H, t; –CH_3), 1.80 (2H, m; –CH_2–), 2.05–2.31 (6H, m; –CH_2–), 4.30 (2H, t; –OCH_2–), 4.55 (2H, t; –NCH_2–), 4.82 (2H, t; –NCH_2–), 7.25 (2H, d; aromatic), 7.74 (9H, m; aromatic), 8.09 (2H, d; aromatic), 8.21 (6H, m; aromatic), 8.72 (2H, d; aromatic), 8.77 (2H, d; aromatic), 8.87–8.88 (8H, m; aromatic), 9.05 (2H, d; aromatic), 9.23 (2H, d; aromatic). Found: C, 59.07; H, 5.58; N, 6.51%; C/N, 9.07. Calcd. for $C_{62}H_{52}N_6OZnBr_2{\cdot}8H_2O$: C, 58.80; H, 5.41; N, 6.64%; C/N, 8.86.

ZnPC$_6$V. Yield: 0.29 g (89.3%). ^{1}H NMR ($CDCl_3$–CD_3OD(9:1, v/v)) δ = 0.97 (3H, t; –CH_3), 1.65 (2H, m; –CH_2–), 1.78–2.23 (8H, m; –CH_2–), 4.29 (2H, t; –OCH_2–), 4.45 (2H, t; –NCH_2–), 4.80 (2H, t; –NCH_2–), 7.25 (2H, d; aromatic), 7.74 (9H, m; aromatic), 8.15 (2H, d; aromatic), 8.21 (6H, m; aromatic), 8.64 (2H, d; aromatic), 8.73 (2H, d; aromatic), 8.87–8.89 (8H, m; aromatic), 8.97 (2H, d; aromatic), 9.24 (2H, d; aromatic). Found: C, 63.00; H, 5.45; N, 6.99%; C/N, 9.01. Calcd. for $C_{63}H_{54}N_6OZnBr_2{\cdot}4H_2O$: C, 62.62; H, 5.17; N, 6.96%; C/N, 9.00.

ZnPC$_7$V. Yield: 0.11 g (33.8%). ^{1}H NMR ($CDCl_3$–CD_3OD(9:1, v/v)) δ = 0.99 (3H, t; –CH_3), 1.54 (2H,

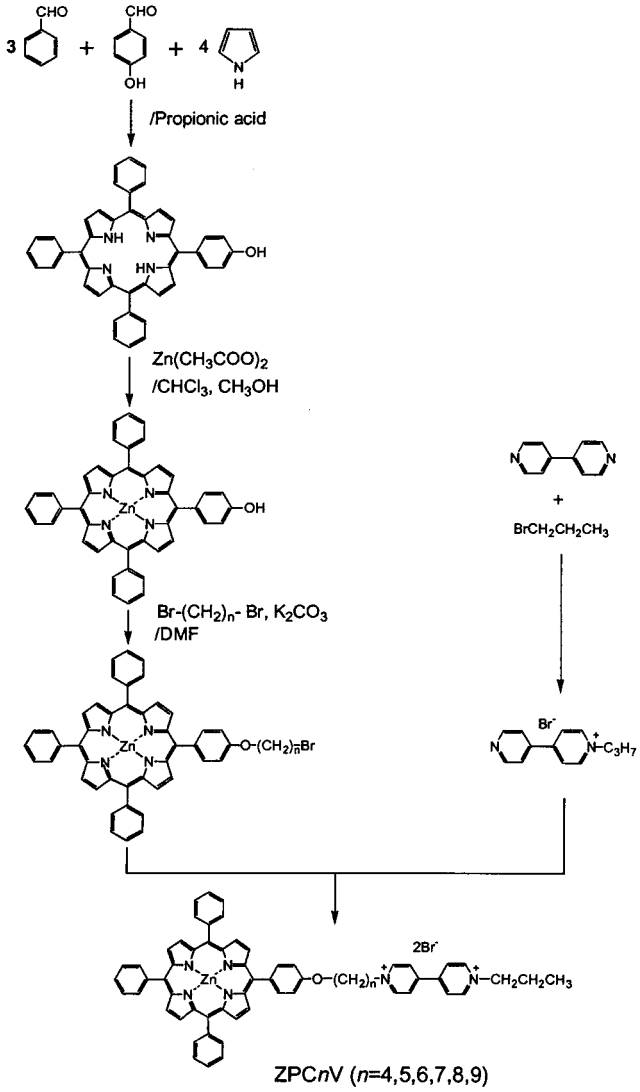

Scheme 1. Syntheses of ZPC$_n$V (n = 4,5, 6, 7, 8, 9).

m; –CH_2–), 1.67–2.15 (10H, m; –CH_2–), 4.27 (2H, t; –OCH_2–), 4.44 (2H, t; –NCH_2–), 4.72 (2H, t; –NCH_2), 7.26 (2H, d; aromatic), 7.75 (9H, m; aromatic), 8.01 (2H, d; aromatic), 8.21 (6H, m; aromatic), 8.54 (2H, d; aromatic), 8.65 (2H, d; aromatic), 8.89 (8H, m; aromatic), 8.90 (2H, d; aromatic), 9.16 (2H, d; aromatic). Found: C, 60.47; H, 5.53; N, 6.69%; C/N, 9.04. Calcd. for $C_{64}H_{56}N_6OZnBr_2 \cdot 7H_2O$: C, 60.21; H, 5.53; N, 6.59%; C/N, 9.14.

ZnPC$_9$V. Yield: 0.33 g (98.8%). ^{1}H NMR ($CDCl_3$-CD_3OD(9:1, v/v)) δ = 1.04 (3H, t; –CH_3), 1.51 (2H, m; –CH_2–), 1.65–2.13 (14H, m; –CH_2–), 4.27 (2H, t; –OCH_2–), 4.58 (2H, t; –NCH_2–), 4.73 (2H, t; –NCH_2–), 7.27 (2H, d; aromatic), 7.74 (9H, m; aromatic), 8.10 (2H, d; aromatic), 8.21 (6H, m; aromatic), 8.60 (2H, d; aromatic), 8.66 (2H, d; aromatic), 8.87–8.91 (8H, m; aromatic), 9.03 (2H, d; aromatic), 9.16 (2H, d; aromatic). Found: C, 62.24; H, 5.72; N, 6.51%; C/N, 9.43. Calcd. for $C_{66}H_{60}N_6OZnBr_2 \cdot 6H_2O$: C, 61.61; H, 5.64; N, 6.53%; C/N, 9.43.

Measurements

UV/Vis absorption spectra were recorded with 10 mm standard quartz cell at 25 ± 0.1 °C. Typical concentrations of ZnPC$_n$V were 2×10^{-4} and 2×10^{-5} M in CH_3CN:H_2O (1:1, v/v). Complex formation constants (K_1 and K_2) with TM-β-CD were obtained from the absorbance change at 25 ± 0.1 °C by the use of non linear least-squares curve fitting method (Marquardt's method) [46].

^{1}H NMR spectra for measurements of the complex formation of ZnPC$_n$V with TM-β-CD were measured at 30 ± 0.2 °C. Concentration of ZnPC$_n$V was 2×10^{-3} M in CD_3CN–D_2O (1:1, v/v), unless otherwise mentioned. Chemical shifts were calculated from a solvent peak (CD_2HCN; δ = 1.913 ppm). Peak assignments of ^{1}H NMR spectra were made by the use of 1D spectra, H-H COSY, and NOESY spectra.

Results and discussion

Syntheses of ZnPC$_n$V

Zinc (II) tetraphenylporphyrin-viologen linked compounds (ZnPC$_n$V, n = 4–9) were synthesized according to the usual methods. The synthetic pathway is summarized in Scheme 1. The abbreviation of the proton in the compounds is shown on the structure in Figure 1.

Dimer formation of ZnPC$_9$V

Several researchers pointed out that the porphyrin derivatives sometimes existed as a dimer in several solvents at high concentration [47, 48]. Then the concentration dependence of the ^{1}H NMR spectra of ZnPC$_n$V was first investigated. Figure 2 shows the concentration effects on the ^{1}H NMR spectra of ZnPC$_9$V in CD_3CN–D_2O (1:1, v/v) as a typical result. In this medium ZnPC$_9$V would exist as an ionic species ZnPC$_9$V^{2+}. At the lowest concentration of ZnPC$_9$V^{2+} (0.1×10^{-3} M), the chemical shifts of protons q and r of the benzene ring which is connected to the oxyalkyl chain are 7.20 and 7.97 ppm, respectively. With the increase of the concentration of this compound, these peaks shifted to higher magnetic fields ($\Delta\delta$ = 0.65 and 0.50 ppm for q and r protons, at 2×10^{-3} M, respectively). Simultaneously, large chemical shift changes were also observed for the methylene protons a and b. The spectral change in Figure 2 clearly indicates that ZnPC$_9$V^{2+} exists as a monomer at lower concentration, while it forms an aggregate at higher concentration. Assuming that this aggregation is a dimer formation at high concentration of ZnPC$_9$V^{2+}, the association equilibrium and the constant (K_a) for dimerization are defined as follows:

$$2\mathrm{ZnPC}_n\mathrm{V}^{2+} \rightleftarrows (\mathrm{ZnPC}_n\mathrm{V}^{2+})_2, \quad (1)$$

$$K_a = [(\mathrm{ZnPC}_n\mathrm{V}^{2+})_2]/[\mathrm{ZnPC}_n\mathrm{V}^{2+}]^2. \quad (2)$$

Here, (ZnPC$_n$V^{2+})$_2$ is a dimer of ZnPC$_n$V^{2+}. If the formation and dissociation rates are faster than the NMR

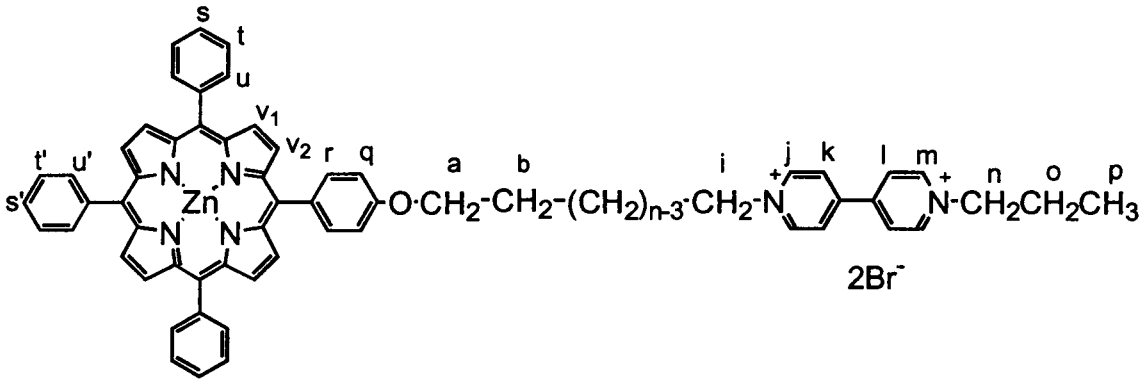

$ZnPC_nV^{2+}$ (n = 4, 5, 6, 7, 8, and 9)

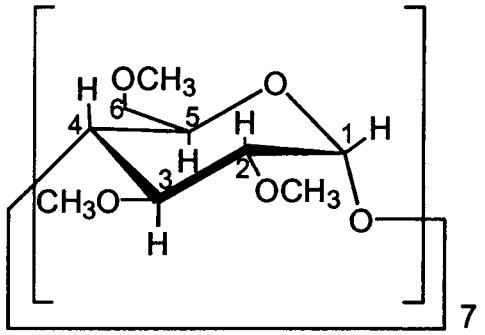

2,3,6-tri-*O*-methyl-β-cyclodextrin

Figure 1. Molecular structures of zinc (II) tetraphenylporphyrin-viologen chain-linked compound ($ZnPC_nV^{2+}$; n = 4–9) and 2,3,6-tri-*O*-methyl-β-cyclodextrin(TM-β-CD). The abbreviation systems for $ZnPC_nV^{2+}$ and TM-β-CD for ^{1}H NMR assignment are shown in the structures.

time scale, the chemical shifts of the monomer and the dimer should be averaged, and one peak is observed. The observed chemical shifts (δ) are calculated as follows [49]:

$$\delta = \frac{\delta_m \cdot [ZnPC_nV^{2+}] + 2\delta_d \cdot [(ZnPC_nV^{2+})_2]}{[ZnPC_nV^{2+}] + 2[(ZnPC_nV^{2+})_2]}. \quad (3)$$

Here, δ_m and δ_d are chemical shifts of the monomer and dimer, respectively. This equation was converted to Equation (4), using a total concentration of $ZnPC_nV^{2+}$.

$$\delta = \frac{\sqrt{1 + 8K_a[ZnPC_nV^{2+}]_t} - 1}{4 \cdot K_a[ZnPC_nV^{2+}]_t}(\delta_m - \delta_d) + \delta_d. \quad (4)$$

Here,

$$[ZnPC_nV^{2+}]_t = [ZnPC_nV^{2+}] + 2[(ZnPC_nV^{2+})_2]. \quad (5)$$

Equation (4) shows that the chemical shifts of $ZnPC_nV^{2+}$ arise from the monomer (δ_m) at low concentration and the dimer (δ_d) at high concentration of $ZnPC_nV^{2+}$.

From these chemical shift changes, the association constant (K_a) for dimerization in CD_3CN–D_2O (1:1, v/v at 30 °C) was calculated to be 80 M^{-1} by the use of a nonlinear least-squares fitting method (Marquardt's method) [46]. The good curve fitting in Figure 3 indicated that the aggregation was a dimer formation of $ZnPC_9V^{2+}$. As limiting chemical shifts of the protons, the chemical shifts of a monomer and a dimer were also calculated. Several data are listed in Table 1.

Quite large high field chemical shift changes of protons q, r and a were observed on dimerization. Small changes of protons b and v_2 were also observed. This fact clearly shows that one porphyrin ring was positioned just above the protons q, r and a of another $ZnPC_9V^{2+}$. A large ring current of the porphyrin caused the high field shifts of these protons. The

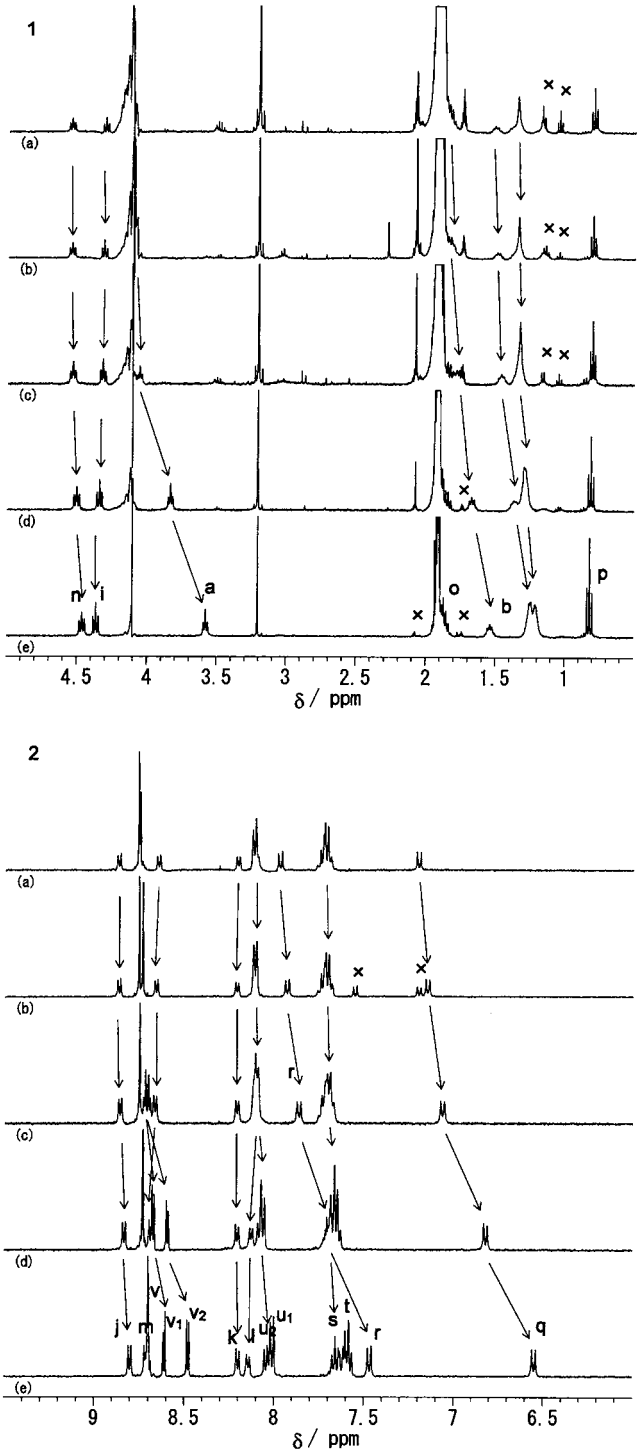

Figure 2. (2-1) ^{1}H NMR spectral change of $ZnPC_9V^{2+}$ at the higher magnetic field in CD_3CN–D_2O (1:1, v/v) at 30 °C as a function of concentration of the $ZnPC_9V^{2+}$; (a) 0.1, (b) 0.2, (c) 0.4, (d) 1.0, and (e) 2.0×10^{-3} M, and (2-2) ^{1}H NMR spectral change of $ZnPC_9V^{2+}$ at the lower magnetic field in CD_3CN–D_2O (1:1, v/v) at 30 °C as a function of concentration of the $ZnPC_9V^{2+}$; (a) 0.1, (b) 0.2, (c) 0.4, (d) 1.0, and (e) 2.0×10^{-3} M.

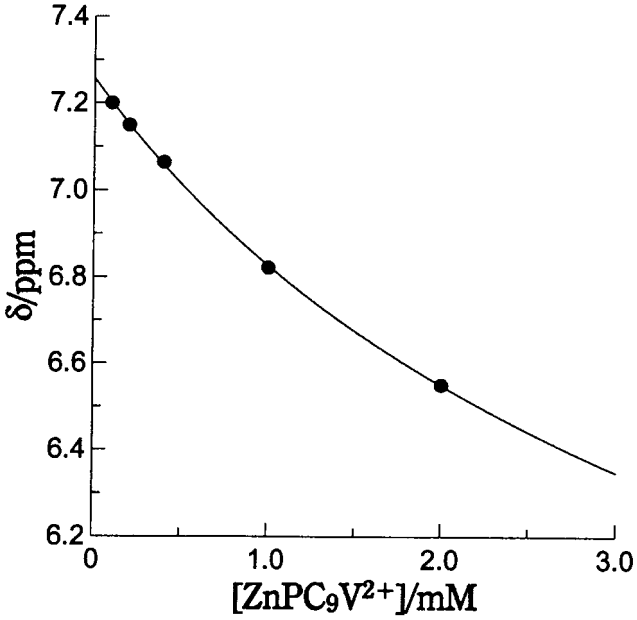

Figure 3. Titration curve of the chemical shift changes of the *q* proton in $ZnPC_9V^{2+}$.

Table 1. Chemical shifts (δ ppm) of the protons of $ZnPC_9V^{2+}$ in monomer and dimer states

Proton	*a*	*b*	*j*	*k*	*l*	*m*	*q*	*r*	v_1	v_2
δ_m	4.23	1.88	8.88	8.21	8.12	8.65	7.26	8.02	8.77	8.80
δ_d	1.01	0.19	8.51	8.15	8.22	8.97	3.77	5.31	8.01	7.13
$\delta_m-\delta_d$	3.22	1.69	0.37	0.06	−0.10	−0.32	3.49	2.71	0.76	1.67

These values were calculated from the observed chemical shifts and an association constant K_a = 80 M^{-1} in CD_3CN–D_2O (1:1, v/v) solution.

plausible structure of this dimer is shown in Figure 4. In this structure, the two porphyrin rings were not overlapped at their centers, and took a slipped face-to-face structure.

It has been reported that many porphyrin derivatives formed a variety of molecular complexes in aqueous solution through noncovalent interactions. Kano *et al.* have reported the dimer formation of several cationic porphyrins in water [47, 48] and large association constants 10^5–10^6 M^{-1} were obtained in water [47]. The small association constant in this experiment is due to the smaller polarity of the solvent (CD_3CN–D_2O) than water. One of the proposed structures can be appraised in this experiment. The present dimer formation is thought to be induced by the hydrophobic interaction of the porphyrin moiety. The association abilities of other $ZnPC_nV^{2+}$ (n = 4–8) may be equal or less than that of $ZnPC_9V^{2+}$, because their hydrophobicity should be less than that of $ZnPC_9V^{2+}$.

Formation of supramolecular complexes of $ZnPC_nV^{2+}$ with TM-β-CD

^{1}H NMR spectra can give good information for the formation of supramolecular complexes. However, we could not obtain any evidence of the formation of supramolecular complexes of $ZnPC_nV^{2+}$ with 2,3,6-tri-*O*-methy-α-

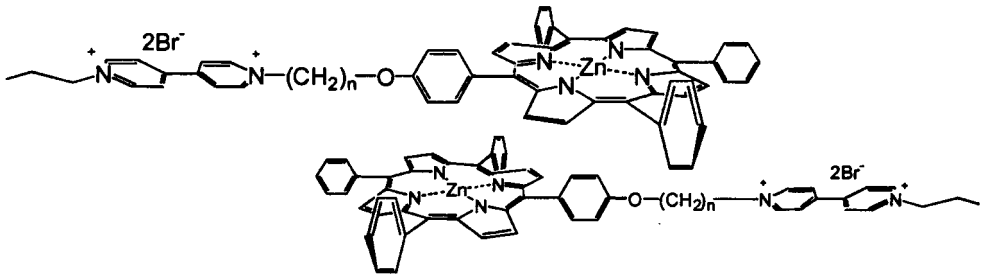

Figure 4. Plausible structure of the dimer of $ZnPC_nV^{2+}$ deduced from the ^1H NMR measurements.

cyclodextrin (TM-α-CD) by the use of ^1H NMR or UV/Visible spectra in methanol, CH_3CN, or CH_3CN–H_2O solvents. This is due to too small a cavity size of TM-α-CD against the benzene or pyridinium ring of $ZnPC_nV^{2+}$. On the other hand, 2,3,6-tri-*O*-methyl-β-cyclodextrin (TM-β-CD) gave quite interesting results.

Figure 5 shows typical ^1H NMR spectra of $ZnPC_9V^{2+}$ in the absence and presence of TM-β-CD. On addition of a small amount of TM-β-CD to $ZnPC_nV^{2+}$ ([TM-β-CD]/[$ZnPC_9V^{2+}$] = 0.4), the methyl protons of –OCH_3(3) in TM-β-CD gave two peaks (2.47 and 2.29 ppm) in the higher field region. No peak corresponding to the –OCH_3(3) of free TM-β-CD (3.48 ppm) was observed. The intensity ratio of the two peaks was ca. 3:1, and this ratio and the peak positions did not change by the addition of TM-β-CD until [TM-β-CD]/[$ZnPC_9V^{2+}$] = 1.0. This result means that two types of complexes were formed and they were quite stable.

Further addition of TM-β-CD gave low magnetic field shift of the lower large peak (2.47 ppm) toward the original peak position (3.48 ppm) of TM-β-CD. Therefore, this peak was assigned to the methyl proton (3) of the complexed TM-β-CD, which takes place by rapid exchange with excess TM-β-CD. The same behavior was also observed for –OCH_3(2). However, the smaller peaks of each –OCH_3(2) and –OCH_3(3) did not change their position. These peaks were assigned to the methyl protons of another type of TM-β-CD complex, which takes place in quite slow exchange ($k_{ex} \leq 40\ s^{-1}$) with excess TM-β-CD. This should be the through-ring (rotaxane) type complex (complex E) as shown in Figure 6, which was also reported for the carbazole-viologen linked compound [35]. The same results were also observed for other protons in TM-β-CD (e.g., H(1) and H(2)).

The chemical shifts of –OCH_3(3) and –OCH_3(2) of the complexes were unusually shifted to high field by the complexation. In particular, the amount of high field shift of –OCH_3(3) was ca. 1.2 ppm and 1.0 ppm for slow and rapid exchanging complexes, respectively. On the other hand, the chemical shift of –OCH_3(6) was little affected by the complexation. Since these high field shifts should be due to the ring current effect of the porphyrin and/or phenyl ring of $ZnPC_9V^{2+}$, the large rim of TM-β-CD where –OCH_3(3) and –OCH_3(2) are positioned faced the porophyrin ring center.

As shown later, since only a 1:1 complex formed in the composition of equal amounts of TM-β-CD and $ZnPC_9V^{2+}$, the fast exchanging complex can be assigned to complex C and D in Figure 6. The exchange rate between complex C and D was quite fast: the protons of the complexes could not be distinguished from each other by ^1H NMR, and the signal intensity was observed as a sum of C and D. The ratio of signal intensities of complex E and the sum of complex C and D was ca. 1:3. Complex D should be counted twice. When statistical effects were considered in this complexation equilibrium, the formation abilities of individual complexes (C, D, and E) may be equal to each other.

As mentioned above, further addition of TM-β-CD did not give a chemical shift change of the small peak (2.29 ppm) of –OCH_3(3), but the peak intensity increased until [TM-β-CD]/[$ZnPC_9V^{2+}$] $\approx$ 2. This fact shows that a higher order complex than 1:1 was formed, and this could be a 2:1 (TM-β-CD: $ZnPC_9V^{2+}$) complex. The ratio of the intensity of –OCH_3(3) (2.29 ppm) against the total intensity of peak q was ca. 2:11, and this means that this type of complex comprised ca. 50% of $ZnPC_9V^{2+}$ complexes.

In the low field region ($\delta > 6$ ppm), interesting changes were observed (Figure 5-2). The proton q, which is on the benzene ring attached to the oxyalkyl chain, showed a characteristic change of its chemical shift. The chemical shift of q shifted to lower magnetic field by the addition of TM-β-CD, until [TM-β-CD]/[$ZnPC_9V^{2+}$] = 1.0. At the same time, a new peak (q') appeared at 7.04 ppm. With the increase of TM-β-CD, the position did not change, but the intensity increased. The low field shift was mainly caused by the decrease of the concentration of uncomplexed $ZnPC_9V^{2+}$ as shown in the previous section. However, the addition of excess TM-β-CD did not move peak q to its monomer position (7.26 ppm), and the peak reached 7.00 ppm at [TM-β-CD]/[$ZnPC_9V^{2+}$]= 1.0. Therefore, the low field shift of peak q also indicates formation of rapid exchanging complexes C and D, and the position was the average of those of the four species: i.e., complex C, D, monomer and dimer of $ZnPC_9V^{2+}$.

The peak height of new peak q' at 7.04 ppm increased on addition of TM-β-CD. This peak intensity was proportional to that of –OCH_3(3) at 2.29 ppm, and the ratio was ca. 2:21 and the ratio of this peak intensity against the higher field peak q was ca. 1:3 at [TM-β-CD]/[$ZnPC_9V^{2+}$] = 1.0. On the basis of the observation, the lower field peak (7.04 ppm) was assigned to the proton q' of the slow exchanging complex (i.e., complex E), and the high field one (q) was the averaged peak of complexes C and D.

Table 2. Second complex formation constant (K_2)[a], peak intensity ratio of –OCH_3(3)/–OCH_3(3′) of the 1:1 complex, and H(q)/H(q') of the 1:2 complex of $ZnPC_nV^{2+}$ with TM-β-CD

n	$K_2/10^3$ M^{-1}	–OCH_3(3)/–OCH_3(3′)[b]	H(q)/H(q')[c]
4	3.7	11.7	4.0
5	3.9	7.2	2.9
6	5.1	4.4	1.8
7	5.6	3.0	1.2
8	5.2	3.0	1.0
9	5.4	3.0	1.0

[a] K_2 values were evaluated by UV/Vis absorption spectra (2×10^{-4} and 2×10^{-5} M).
[b] The value –OCH_3(3)/–OCH_3(3′) corresponds to the concentration ratio of the sum of complex C, D_1 and D_2 vs. complex E.
[c] The value H(q)/H(q') corresponds to the concentration ratio of the complex F vs. complex G.

Further addition of TM-β-CD ([TM-β-CD]/[$ZnPC_9V^{2+}$] > 1) gave a high field shift on q, contrary to the case of a small addition of TM-β-CD. This high field shift reached the position of 6.96 ppm on addition of [TM-β-CD]/[$ZnPC_9V^{2+}$] > 3. On the other hand, the lower field peak q' did not change its position, and the height increased. The maximum intensity ratio of q':q was ca. 1:1. This fact also indicates the formation of two types of 2:1 complex (TM-β-CD:$ZnPC_9V^{2+}$), and the ratio of populations of the complexes was ca. 1:1. The plausible structures of these two types of complexes were complex F and G as shown in Figure 6. The same behavior of complexation of other $ZnPC_nV^{2+}$ with TM-β-CD were also observed except for $ZnPC_4V^{2+}$.

The peak intensity ratio of –OCH_3(3) vs. –OCH_3(3′) of $ZnPC_4V^{2+}$ was ca. 1:9 (Table 2). This means the ratio of the amounts of complex E vs. complex C and D was 1:9, because only the exchange rate for complex E is as slow as $ZnPC_9V^{2+}$. If the same consideration to $ZnPC_9V^{2+}$ was adopted to this result, the formation ability of complex E was one third of those of complex C and D.

Complexation constants of $ZnPC_nV^{2+}$ with TM-β-CD

Absorption spectral experiments of $ZnPC_nV^{2+}$ ($n = 9$) in the presence of TM-β-CD were carried out. Two main absorption peaks of the Q-band around 560 and 598 nm shifted to shorter wavelength by the addition of TM-β-CD. Coincidently, the peak height at shorter wavelength increased and that at longer wavelength decreased. In contrast, the peak shift of the Soret band around 422.5 nm was small on addition of TM-β-CD. The same trends were observed for other $ZnPC_nV^{2+}$. In consideration of the results of NMR spectra, these spectral changes reflected the formation of supramolecular complexes of $ZnPC_9V^{2+}$ with TM-β-CD.

When adding TM-β-CD gradually, the absorbance of $ZnPC_9V^{2+}$ at 598.5 nm (second peak max.) decreased linearly until the ratio of TM-β-CD was 1:1, and beyond a 1:1 ratio the decrease of the absorbance was slower and not linear as shown in Figure 7. On the basis of NMR data, we have assumed that encapsulation proceeds via a two-step binding process (Figure 6). However, the discrete formation of com-

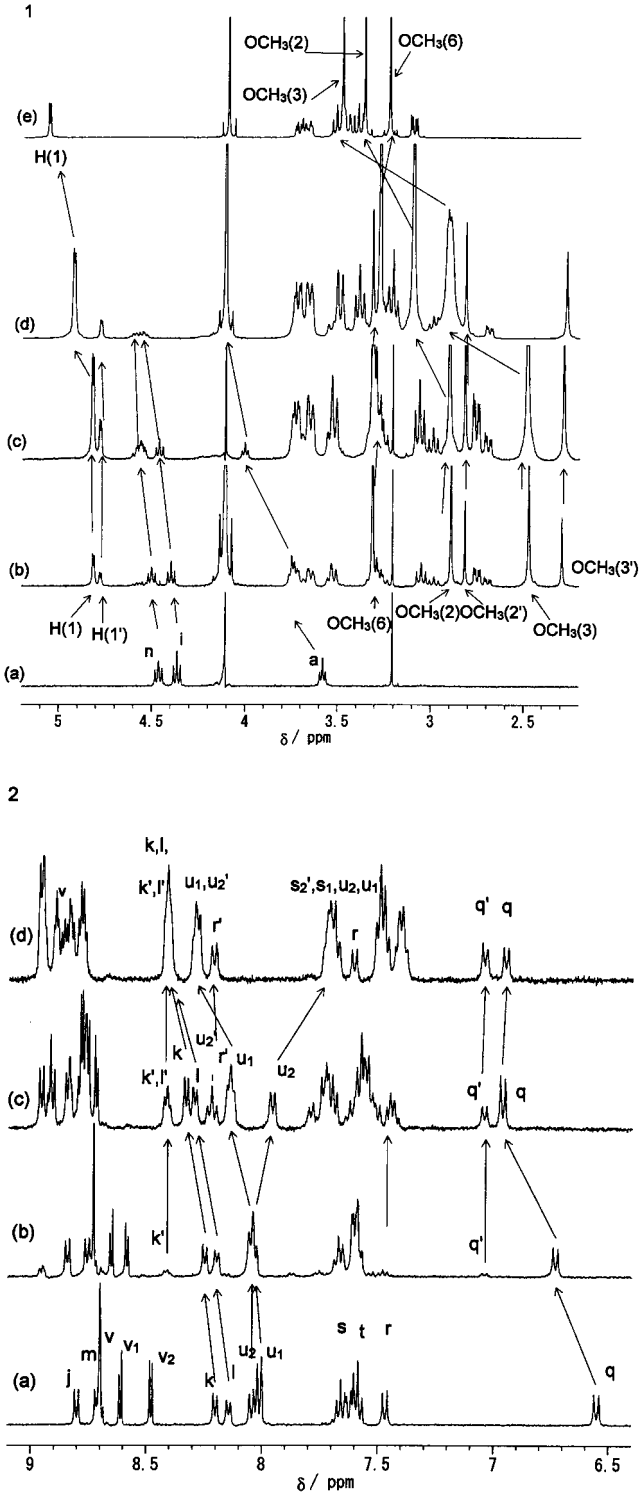

Figure 5. (5-1) ^{1}H NMR spectra of $ZnPC_9V^{2+}$ (2×10^{-3} M) in higher magnetic field on adding TM-β-CD ((a) 0 M, (b) 0.4×10^{-3} M, (c) 2.4×10^{-3} M, (d) 7.2×10^{-3} M, and (e) TM-β-CD only) in CD_3CN–D_2O (1:1, v/v) at 30 °C, and (5-2) ^{1}H NMR spectra of $ZnPC_9V^{2+}$ (2×10^{-3} M) in lower magnetic field on adding TM-β-CD ((a) 0 M, (b) 0.4×10^{-3} M, (c) 2.4×10^{-3} M, (d) 7.2×10^{-3} M) in CD_3CN–D_2O (1:1, v/v) at 30 °C.

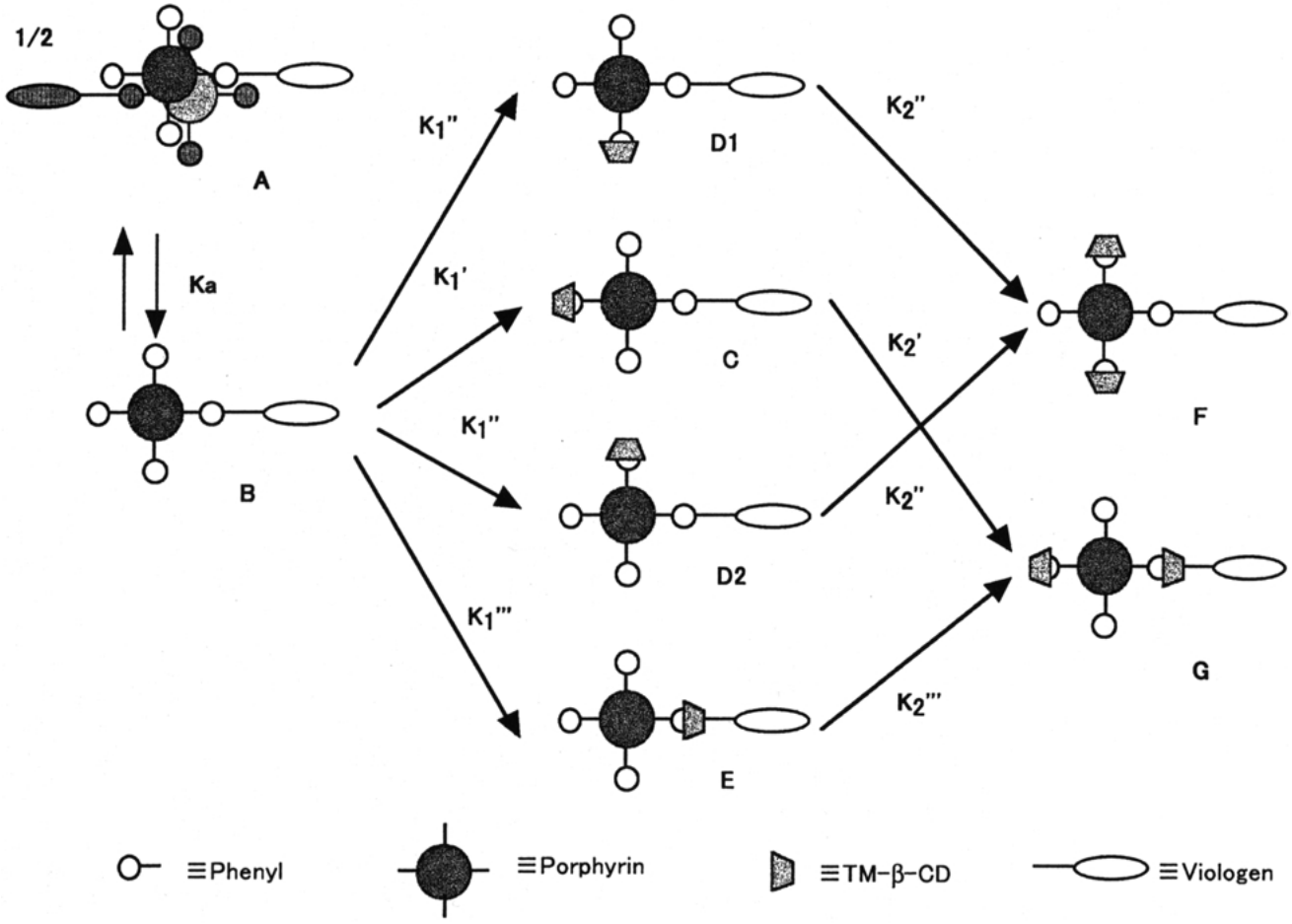

Figure 6. Schematic representation of the kinetics of the supramolecular complex formation of $ZnPC_nV^{2+}$ with TM-β-CD. K_a is an association constant for dimerization, K_1 and K_2 are apparent complex formation constants with TM-β-CD for 1:1 and 1:2 complexes.

plex C, D and E and also that of complex F and G cannot be distinguished from the absorption spectra. Since the relative ratios of complex C, D and E are always constant, the complex C, D and E could be thought to be one species as a 1:1 complex, i.e., $ZnPC_nV^{2+}$·(TM-β-CD), and also the complex F and G was a 1:2 complex, i.e., $ZnPC_nV^{2+}$·(TM-β-CD)$_2$.

Consequently, the complexation equilibria of $ZnPC_nV^{2+}$ and TM-β-CD are defined as follows:

$$ZnPC_nV^{2+} + \text{TM-}\beta\text{-CD} \rightleftarrows ZnPC_nV^{2+} \cdot \text{TM-}\beta\text{-CD}, \quad (6)$$

$$ZnPC_nV^{2+} \cdot \text{TM-}\beta\text{-CD} + \text{TM-}\beta\text{-CD} \rightleftarrows ZnPC_nV^{2+} \cdot (\text{TM-}\beta\text{-CD})_2. \quad (7)$$

The complex formation constants, K_1 and K_2, are defined as Equations (8) and (9) for the equilibria (6) and (7), respectively

$$K_1 = \frac{[ZnPC_nV^{2+} \cdot \text{TM-}\beta\text{-CD}]}{[ZnPC_nV^{2+}][\text{TM-}\beta\text{-CD}]}, \quad (8)$$

$$K_2 = \frac{[ZnPC_nV^{2+} \cdot (\text{TM-}\beta\text{-CD})_2]}{[ZnPC_nV^{2+} \cdot \text{TM-}\beta\text{-CD}][\text{TM-}\beta\text{-CD}]}, \quad (9)$$

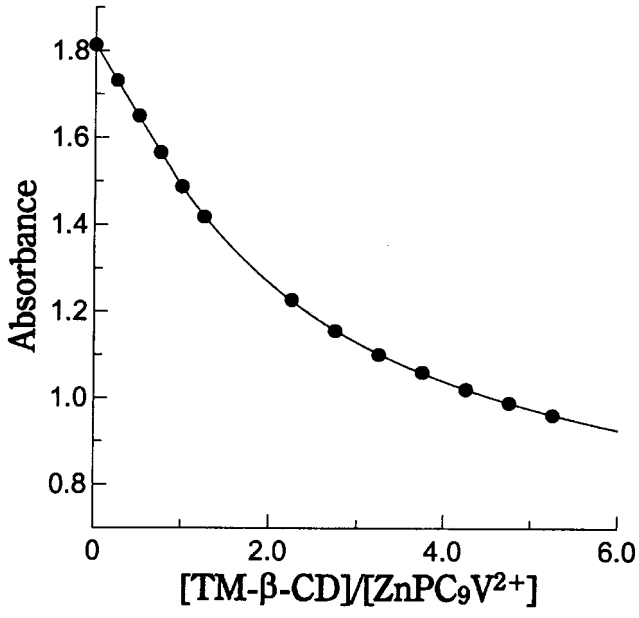

Figure 7. Titration curve of the absorbance of $ZnPC_9V^{2+}$ at 598.5 nm on addition of TM-β-CD. $[ZnPC_9V^{2+}] = 2 \times 10^{-4}$ M.

$$\text{Abs.} = \epsilon_1[\text{ZnPC}_n\text{V}^{2+}] + \epsilon_2[\text{ZnPC}_n\text{V}^{2+} \cdot \text{TM-}\beta\text{-CD}] + \\ + \epsilon_3[\text{ZnPC}_n\text{V}^{2+} \cdot (\text{TM-}\beta\text{-CD})_2]. \quad (10)$$

Here, ϵ_1, ϵ_2 and ϵ_3 are the absorption coefficients for free $\text{ZnPC}_n\text{V}^{2+}$, 1:1 and 1:2 complexes, respectively. If the absorption coefficients of these species are different from each other, the formation constants K_1 and K_2 can be evaluated from the absorbance change. The most significant change was observed at 598.5 nm for all $\text{ZnPC}_n\text{V}^{2+}$. Thus, the evaluation of the formation constants $K_{1,2}$ was carried out at this wavelength using the Marquardt curve-fitting method [46] according to Equations (8), (9), and (10) as shown in Figure 7.

In all cases, the small but almost linear absorbance change was observed until a 1:1 ratio of TM-β-CD against $\text{ZnPC}_n\text{V}^{2+}$. Since the use of any value of more than 10^5 M^{-1} for K_1 was able to fit the observed data, accurate K_1 values could not be evaluated. Thus, K_1 values were estimated to be more than 10^5 M^{-1}. However, the second complexation constants (K_2) of each complex could be evaluated from the curvefitting, and the data are listed in Table 2.

Discrete complex formation constants can be evaluated from the combination with ^{1}H NMR data. The discrete complex formation constants K_1', K_1'' and K_1''' for the 1:1 complex, and K_2', K_2'' and K_2''' for the 1:2 complex as shown in Figure 6 are defined as follows:

$$K_1' = \frac{[C]}{[B][\text{TM-}\beta\text{-CD}]}, \quad (11)$$

$$K_1'' = \frac{[D_1]}{[B][\text{TM-}\beta\text{-CD}]} = \frac{[D_2]}{[B][\text{TM-}\beta\text{-CD}]}, \quad (12)$$

$$K_1''' = \frac{[E]}{[B][\text{TM-}\beta\text{-CD}]}, \quad (13)$$

$$K_1 = \frac{[C] + [D_1] + [D_2] + [E]}{[B][\text{TM-}\beta\text{-CD}]} = K_1' + 2K_1'' + K_1''', \quad (14)$$

$$K_2' = \frac{[G]}{[C][\text{TM-}\beta\text{-CD}]}, \quad (15)$$

$$K_2'' = \frac{[F]}{[D_1][\text{TM-}\beta\text{-CD}]} = \frac{[F]}{[D_2][\text{TM-}\beta\text{-CD}]}, \quad (16)$$

$$K_2''' = \frac{[G]}{[E][\text{TM-}\beta\text{-CD}]}, \quad (17)$$

$$K_2 = \frac{[F] + [G]}{([C] + [D_1] + [D_2] + [E])[\text{TM-}\beta\text{-CD}]}, \quad (18)$$

Here, the following equations exist:

$$K_1 = K_1' + 2K_1'' + K_1''', \quad (19)$$

Table 3. Discrete complex formation constants of $\text{ZnPC}_n\text{V}^{2+}$ with TM-β-CD[a]

n	K_1'/K_1	K_1''/K_1	K_1'''/K_1	$K_2'/10^3$ M^{-1}	$K_2''/10^3$ M^{-1}	$K_2'''/10^3$ M^{-1}
4	0.31	0.31	0.08	2.4	9.7	9.4
5	0.29	0.29	0.12	3.4	9.9	9.4
6	0.27	0.27	0.19	6.7	12.1	9.8
7	0.25	0.25	0.25	11.2	11.2	11.2
8	0.25	0.25	0.25	10.4	10.4	10.4
9	0.25	0.25	0.25	10.8	10.8	10.8

[a]Actual K_1', K_1'' and K_1''' values were not obtained because K_1 values are unknown.

$$K_1 \cdot K_2 = K_1' \cdot K_2' + K_1'' \cdot K_2'', \quad (20)$$

$$K_1''' \cdot K_2''' = K_1' \cdot K_2'. \quad (21)$$

To calculate these constants, the following ratios (R_1 and R_2) are defined, which correspond to the ratio of peak intensity –OCH_3(3)/–OCH_3(3') and H(q)/H(q') as given in Table 2, respectively.

$$R_1 = \frac{[C] + [D_1] + [D_2]}{[E]}, \quad (22)$$

$$R_2 = \frac{[F]}{[G]}. \quad (23)$$

Since complex C, D_1 and D_2 could not be distinguished from each other by ^{1}H NMR spectra, K_1' and K_1'' can not be resolved. However, we can assume that K_1' and K_1'' will be equal, because the steric effect from the viologen moiety will be negligible for these values.

Using this assumption, the concentrations $[C]$, $[D_1]$ and $[D_2]$ could be equal to each other at any time, and K_1', K_1'' and K_1''' can be described as follows:

$$K_1' = K_1'' = \frac{R_1}{3(1 + R_1)} \cdot K_1, \quad (24)$$

$$K_1'' = \frac{1}{(1 + R_1)} \cdot K_1. \quad (25)$$

In the same way, K_2', K_2'', and K_2''' can be also described as:

$$K_2' = \frac{3(1 + R_1)}{R_1(1 + R_2)} \cdot K_2, \quad (26)$$

$$K_2'' = \frac{3R_2(1 + R_1)}{R_1(1 + R_2)} \cdot K_2, \quad (27)$$

$$K_2''' = \frac{(1 + R_1)}{(1 + R_2)} \cdot K_2. \quad (28)$$

Thus, K_2', K_2'', and K_2''' were evaluated from the data in Table 2, and are listed in Table 3.

Since the K_1 values were not obtained in these experiments, the absolute values of K_1', K_1'', and K_1''' could not be calculated. The ratios of these values against K_1 could be calculated according to Equations (24) and (25), and are listed in Table 3.

The K_2 values of the complexes increased with the methylene chain length, and reached a constant value (ca. 5.5×10^3 M^{-1}) over $n = 7$. However, the discrete formation constants K_2'', and K_2''' were little affected by the methylene chain length. Only K_2' exhibits a dependence of the methylene chain length. The small values of K_2' for $n = 4 \sim 6$ are caused by a repulsive interaction between penetrated TM-β-CD and the viologen unit at the second complexation. This repulsive interaction may be a steric and/or hydrophilic (viologen)-hydrophobic (TM-β-CD) interaction. The almost constant values of K_2'' and K_2''' for all compounds show a small interaction between unpenetrated TM-β-CD and the viologen unit.

Although the discrete K_1 values (K_1', K_1'' and K_1''') were not obtained, the ratio of these values shows the same tendency as the discrete K_2 values. Only K_1'''/K_1 exhibits a dependence of the chain length. This is due to the same formation process of complex E as the complex G from C.

References

1. M.L. Bender and M. Komiyama: *Cyclodextrin Chemistry*, Springer-Verlag, New York (1978).
2. 'Cyclodextrins', *Chem. Rev.* **98** (1998).
3. I. Tabushi, K. Fujita, and L.C. Yuan: *Tetrahedron Lett.* **18**, 2503 (1977).
4. D.C. Neckers and J. Paczkowski: *J. Am. Chem. Soc.***108**, 291 (1986).
5. D.C. Neckers and J. Paczkowski: *Tetrahedron* **42**, 4671 (1986).
6. M.C. Gonzalez, A.R. McIntosh, J.R. Bolton, and A.C. Weedon: *J. Chem. Soc.*, *Chem. Commun.* 1138 (1984).
7. A.M, Aquino, C.J. Abelt, K.L. Berger, C.M. Darragh, S.E. Kelly, and M.V. Cossette: *J. Am. Chem. Soc.* **112**, 5819 (1990).
8. B.K. Hubbard, L.A. Beilstein, C.E. Heath, and C.J. Abelt: *J. Chem. Soc.*, *Perkin Trans. 2*, 1005 (1996).
9. A. Nakamura, S. Okutsu, Y. Oda, A. Ueno, and F. Toda: *Tetrahedron Lett.* **35**, 7241 (1994)
10. D.L. Dick, T.V.S. Rao, D. Sukumaran, and D.S. Lawrence: *J. Am. Chem. Soc.* **114**, 2664 (1992).
11. T. Jiang and D.S. Lawrence: *J. Am. Chem. Soc.* **117**, 1857 (1995).
12. F. Venema, A.E. Rowan, and R.J.M. Nolte: *J. Am. Chem. Soc.* **118**, 257 (1996).
13. S. Mosseri, J.C. Mialocq, B. Perly, and P. Hambright: *J. Phys. Chem.* **95**, 2196 (1991).
14. G.L, Closs and J.R. Miller: *Science* **240**, 440 (1988).
15. M.R. Wasielewski: *Chem. Rev.* **92**, 435 (1992).
16. D. Gust, T.A. Moore, and A.L. Moore: *Acc. Chem. Res.* **26**, 198 (1993).
17. N.J. Turro: in B. Cummings (ed.), *Modern Molecular Photochemistry*, Menlo Park (1978).
18. G.J. Kavarnos and N.J. Turro: *Chem. Rev.* **86**, 401 (1986).
19. U.E. Steiner and T. Ulrich: *Chem. Rev.* **89**, 51 (1989).
20. H. Hayashi: in J.F. Rabek (ed.), *Photochemistry and Photophysics*, CRC Press, Boca Raion, Vol. I (1990), p. 59.
21. H. Nakamura, A Uehata, A. Motonaga, T. Ogata, and T. Matsuo: *Chem. Lett.* 543 (1987).
22. A. Uehata, H. Nakamura, S. Usui, and T. Matsuo: *J. Phys. Chem.* **93**, 8197 (1989).
23. T. Ito, M. Naka, A. Miura, T. Ujiie, H. Nakamura, and T. Matsuo: *Bull. Chem. Soc. Jpn.* **74**, 657 (2001).
24. V.Ya. Shafirovich, E.E. Batova, and P.P. Levin: *Chem. Phys. Lett.* **210**, 101 (1993).
25. T. Ito, T. Ujiie, M. Naka, and H. Nakamura: *Chem. Phys. Lett.* **340**, 308 (2001).
26. M.C.T. Fyfe and J.F. Stoddart: *Acc. Chem. Res.* **30**, 393 (1997).
27. G. Wenz: *Angew. Chem. Int. Ed. Engl.* **33**, 803 (1994).
28. A. Harada, J. Li, and M. Kamachi: *Nature* **356**, 325 (1992).
29. H. Ogino: *New. J. Chem.* **17**, 683 (1993).
30. S.A. Nepogodiev and J.F. Stoddart: *Chem. Rev.* **98**, 1959 (1998).
31. H. Yonemura, H. Saito, S. Matsushita, H. Nakamura, and T. Matsuo: *Tetrahedron Lett.* **30**, 3143 (1989).
32. H. Yonemura, H. Nakamura, and T. Matsuo: *Chem. Phys. Lett.* **155**, 157 (1989).
33. H. Yonemura, H. Nakamura, and T. Matsuo: *Chem. Phys. Lett.* **162**, 69 (1992).
34. Y. Fujiwara, T. Aoki, K. Yoda, H. Cao, H. Mukai, T. Haino, Y. Fukazawa, Y. Tanimoto, H. Yonemura, T. Matsuo, and M. Okazaki: *Chem. Phys. Lett.***259**, 361 (1996).
35. H. Yonemura, M. Kasahara, H. Saito, H. Nakamura, and T. Matsuo: *J. Phys. Chem.* **96**, 5765 (1992).
36. H. Yonemura, T. Nojiri, and T. Matsuo: *Chem. Lett.* 2097 (1994).
37. A. Toki, H. Yonemura, and T. Matsuo: *Bull. Chem. Soc. Jpn.* **66**, 3382 (1993).
38. E.H. Yonemoto, G.B. Saupe, R.H. Schmehl, S.M. Hubig, R.L. Riley, B.L. Iverson, and T.E. Mallouk: *J. Am. Chem. Soc.* **116**, 4786 (1994).
39. J.W. Park, B.A. Lee, and S.Y. Lee: *J. Phys. Chem. B* **102**, 8209 (1998).
40. F.M. Menger and M. A. Dulany: *Tetrahedron Lett.* 267 (1985).
41. B. Casu, M. Reggiani, G.G. Gallo, and A. Vigevani: *Tetrahedron* **24**, 803 (1968).
42. B. Casu, M. Reggiani, and G.R. Sanderson: *Carbohydr. Res.* **76**, 59 (1979).
43. N. Sakairi and H. Kuzuhara: *Carbohydr. Res.* **266**, 139 (1996).
44. K. Kano, N. Tanaka, H. Minamizono, and Y. Kawakita: *Chem. Lett.* 925 (1996).
45. J.S. Manka and D.S. Lawrence: *Tetrahedron Lett.* **30**, 7341 (1989).
46. D.W. Marquardt: *J. Soc. Ind. Appl. Math.* **11**, 431 (1963).
47. K. Kano, H. Minamizono, T. Kitae, and S. Negi: *J. Phys. Chem. A* **101**, 6118 (1997).
48. K. Kano, K. Fukuda, H. Wakami, R. Nishiyabu, and R.F. Pasternack: *J. Am. Chem. Soc.* **122**, 7494 (2000).
49. J. Sandström: *Dynamic NMR Spectroscopy*, Chapter 2, Academic Press, London (1982).